Magnetocaloric effect in high Gd content Gd-Fe-Al based amorphous/nanocrystalline systems with enhanced Curie temperature and refrigeration capacity

Linlin Zhang,[1,2] Mingdong Bao,[2] Qiang Zheng,[2,a] Linhai Tian,[1,a] and Juan Du[3,a]
[1]*Research Institute of Surface Engineering, Taiyuan University of Technology, Taiyuan City 030024, People's Republic of China*
[2]*School of Materials Science and Chemical Engineering, Ningbo University of Technology, Ningbo, 315016, People's Republic of China*
[3]*Key Laboratory of Magnetic Materials and Devices, Ningbo Institute of Material Technology and Engineering, Chinese Academy of Sciences, 1219 Zhongguan West Road, Ningbo 315201, People's Republic of China*

The Gd-Fe-Al amorphous/nanocrystalline composites were successfully designed and obtained with both high Curie temperature (T_c) and large magnetic entropy change (ΔS_M). The T_c can be tuned from 172 to 280 K and refrigeration capacity (RC) has a value between 690 and 867 J/kg under a field change of 0–5 T by changing the Gd contents and the formation of Gd nanocrystallites. And, ΔS_M in Gd-Fe-Al amorphous/nanocrystalline composites reached a value of 7.2 J kg^{-1} K^{-1} under a field change of 0–5 T. The high RC in Gd-Fe-Al system were ascribed to the widening full width at half maximum (δ_{FWHM}) up to 240 K of the magnetic entropy change (ΔS_M^{max}) peak because of the combination contribution of amorphous matrix and the precipitated Gd-riched nanocrystalline. Our research would shed light on how to design attractive candidates for magnetic refrigeration materials with high performance at near room temperature. [http://dx.doi.org/10.1063/1.4945407]

I. INTRODUCTION

Magnetic refrigeration based on magnetocaloric effect (MCE) has attracted increasing attention because of its superior properties, such as high energy efficiency and environmental friendliness. Therefore, it is expected to replace traditional vapor-compression refrigeration in the near future.[1] For a magnetic refrigeration material, a high magnetic entropy change, ΔS_M, is important for its application on the point of large adiabatic temperature change. Currently, the large MCE has been extensively studied on various crystalline materials with a first-order magnetic transition, such as $La(Fe_{1-x},Si_x)_{13}$,[2,3] $Gd_5Si_2Ge_2$,[4] MnFe(P,As),[5] Ni-Mn-X (X = Sn, In, Sb),[6–8] etc. The advantage of these crystalline materials is their large magnetic entropy change. However, due to the first-order magnetic transition, the thermal and magnetic hysteresis is intrinsically unavoidable. Also, the temperature range of full width at half maximum (δ_{FWHM}) of the magnetic entropy change (ΔS_M^{max}) peak is only a few to a few tens Kelvin. Therefore, the refrigeration capacity in crystalline materials is small.

The amorphous materials undergo second order magnetic transition which will broaden magnetic entropy change (ΔS_m) peaks and result in high values of refrigeration capacity (RC).[9–13] They

[a]Corresponding author: qiangzheng616@hotmail.com (Q. Zheng) dujuan@nimte.ac.cn (J. Du) tlinhai@hotmail.com (L.H.Tian)

also have some unique properties that are superior to those of crystalline alloys, such as, no thermal and field hysteresis, large electrical resistivity, high corrosion resistance, tailorable magnetic transition temperature, fine molding and processing behavior. These characteristics are technically important for the use of amorphous materials as more suitable candidates in magnetic refrigeration applications. The negative point of amorphous materials is their lower Curie temperatures and lower magnetic entropy change compared to those of their crystalline counterparts, which are important factors need to be solved before their real application as refrigeration materials at room temperature.

Recently, many efforts have been devoted to improving Curie temperatures and magnetic entropy change of amorphous materials in Gd-RE (RE = Fe, Co, Ni)-Al systems.[14–18] Most of the research focused on the magnetocaloric effect at low temperature. Unfortunately, there are still no amorphous materials having a Curie temperature close to room temperature combined with a high magnetic entropy change under a magnetic field change (5 T). To circumvent this problem, i.e., obtain both high Curie temperature and large magnetic entropy change, in this work, Gd-based amorphous (Am.) and nanocrystalline (NC) composites are designed based on the idea of combination effect of amorphous and nanocrystalline composites in which the amorphous part contributes to the wide temperature range of δ_{FWHM} and the nanocrystalline part gives high magnetic entropy change. In this paper, the magnetic properties and evolution of magnetocaloric effect of $Gd_x(Fe_{0.566}Al_{0.434})_{100-x}$(x = 65-90) alloys was systematically investigated. As a result, T_c has been tuned to near room temperature in Am./NC composites together with a high ΔS_m and RC. From the best of our knowledge, the RC (867 J/kg) obtained for amorphous and nanocrystalline composites is the highest for all crystalline and amorphous magnetocaloric effect materials. The reason of high Curie temperature and large magnetic entropy change was discussed and explained.

II. EXPERIMENTAL

Master alloys of $Gd_x(Fe_{0.566}Al_{0.434})_{100-x}$(x = 65-90) (atomic percent) were prepared by arc-melting a mixture of pure Gd, Fe and Al metals in a titanium-gettered argon atmosphere. The purities of all raw elements are better than 99.9%. To guarantee the composition homogeneity, each ingot was repeatedly melted five times. The amorphous ribbons with a thickness of about 20 μm and a width of about 2 mm were produced by melt-spinning technology on a singe-roller copper wheel with a speed of 40 m/s.The structure of the as-quenched ribbons was examined by X-ray diffraction (XRD) using Cu-K_α radiation. The thermal properties were investigated by differential scanning calorimetry (DSC) at a constant heating rate of 40 K/min under purified argon atmosphere. The samples were contained in aluminum pans. A second run under identical conditions was used to determine the baseline after each run. To confirm the reproducibility of the experimental results, at least three samples were measured for each composition. All measurements for the glass transition temperature (T_g) and the onset temperature of crystallization (T_x) were reproducible within the error of ±1 K. The magnetic properties were measured by superconducting quantum interference device magnetometer (SQUID). The magnetocaloric effect was studied using Maxwell relations by constructing the temperature dependence of ΔS_M from the isothermal magnetization curve.

III. RESULTS AND DISCUSSIONS

Figure 1(a) shows the X-ray diffraction patterns of $Gd_x(Fe_{0.566}Al_{0.434})_{100-x}$ (x = 65-90) ribbons. The as-spun ribbons have only broad diffused diffraction peaks and no any crystalline peaks can be detected within the resolution of XRD in samples with x = 65, 70, and 73.5, which indicates an amorphous structure in these ribbons. However, obvious crystalline peaks indexed as Gd_3Al_2 and Gd phases can be seen in samples with x = 80 and x = 90, which reveals the presence of nanocrystallines. The grain size of Gd_3Al_2 and Gd was calculated by Debye-Scherrer formula. And, the average size of Gd_3Al_2 and Gd was approximately 20 nm and 28 nm, respectively. The differential scanning calorimetry was used to study the thermal properties of as-spun ribbons. The continuous DSC traces obtained from the $Gd_x(Fe_{0.566}Al_{0.434})_{100-x}$(x = 65-90) at a heating rate of 40 K/min are shown in Figure 1(b). The glass transition can be sheltered by the DSC background

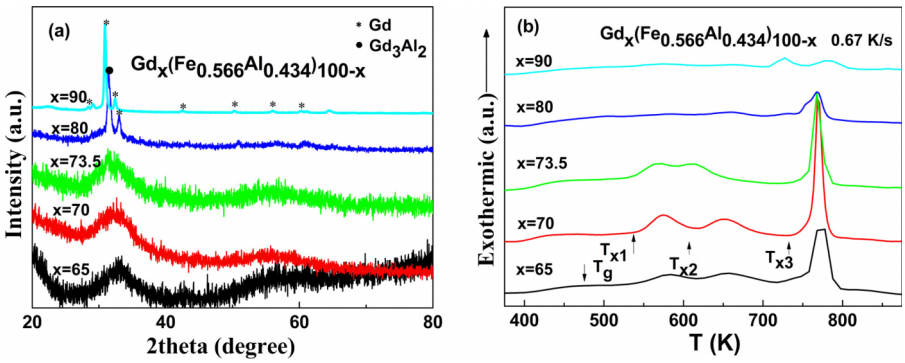

FIG. 1. (a) X-ray diffraction patterns of as-quenched $Gd_x(Fe_{0.566}Al_{0.434})_{100-x}$(x = 65-90) ribbons and (b) DSC curves for as-quenched $Gd_x(Fe_{0.566}Al_{0.434})_{100-x}$(x = 65-90) ribbons.

noise. To eliminate the background noise in DSC measurement, a refined DSC measurement was performed. The same ribbon was measured twice, firstly, in the amorphous state and secondly after crystallization was complete. The DSC curves of $Gd_x(Fe_{0.566}Al_{0.434})_{100-x}$ (x = 65-73.5) alloy show distinct endothermic glass transition before several exothermic crystallization reactions. However, no glass transition phenomenon is seen in the temperature range below crystallization temperature for x = 80 and 90, which indicates that the glass transition temperature (T_g) is estimated to be higher than T_x.

Figure 2 presents the temperature dependence of magnetization of $Gd_x(Fe_{0.566}Al_{0.434})_{100-x}$(x = 65-90) ribbons under an applied field of 200 Oe. The Curie temperatures (T_c), which are defined as the temperature at the maximum of $|dM/dT|$, where M is magnetization and T is temperature, is shown in the inset of Fig. 2. For x = 65, 70 and 73.5, $|dM/dT|$ displays only one maximum originating from the glassy ribbons. However, for x = 80 and x = 90, there are obviously two maxima which indicates the appearance of multiple Curie temperatures. The higher Curie temperature should be ascribed to the ferromagnetic transition of the nanocrystallites.[12] With the increase of temperature, the magnetization (Figure 2) decreases, resulting from the magnetic transition from a ferromagnetic (FM) ordered state to a paramagnetic (PM) ordered state. For the as spun ribbons having only glassy phase without any nanocrystallites, T_c is dominantly determined by the ferromagnetic Fe-Fe exchange interaction.[13,14] Hence, an increase in Fe concentration will result in an increase of T_c from 172 K to 192 K in $Gd_x(Fe_{0.566}Al_{0.434})_{100-x}$ (x = 65-73.5) alloys. However, T_c of $Gd_x(Fe_{0.566}Al_{0.434})_{100-x}$ (x = 80,90) amorphous/nanocrystalline system is very sensitive to the composition and the formation of nanocrystallites. After the precipitation of Gd-riched nanoparticles, the Fe concentration in the amorphous matrix increased. Therefore, T_c in amporphous matrix increased to 206 and 212 K for samples with x = 80 and 90, respectively. And, the second T_c

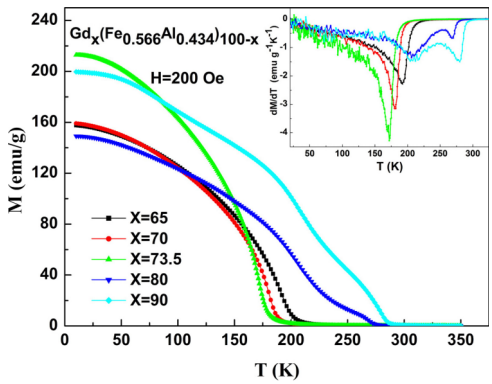

FIG. 2. Temperature dependence of the magnetization of $Gd_x(Fe_{0.566}Al_{0.434})_{100-x}$(x = 65-90) ribbons under an applied field of 200 Oe. The inset shows the derivative curves of dM/dT vs. T.

(second maxima in the inset of Fig. 2) was ascribed to the precipitated Gd-riched nanocrystalline phase, Gd and/or Gd_3Al_2.

In Fig. 2, at the lowest temperature the x = 65 and 70 samples have a magnetization of about 160 emu/g, while the x = 73.5 sample goes up to almost 220 emu/g. The possible reason may be the fully amorphous nature of samples x = 65 and 70, while it has inhomogeneous structure in atomic scale for x = 73.5 sample, even if it is amorphous within XRD resolution. For example, it was reported that Gd-Fe-Al amorphous alloy was obtained according to XRD results, however there was Fe-rich clusters existing in Gd-Fe-Al amorphous matrix proved by the high resolution transmission electron microscopy (HRTEM) in Ref. 19. In other words, x = 73.5 sample is fully amorphous from XRD patterns. However, it may be atomically inhomogeneous like that in Ref. 19. On the other side, due to the precipitation of Fe-rich clusters, the content of Gd will increase, and the Gd-Gd interaction will increase, and this will also induce the high magnetization. Additionally, in Refs. 14–16, no amorphous alloy having Gd content more than 70 % was obtained. Then for x = 80 sample, magnetization drops to about 150 emu/g because of the precipitation of nanocrystalline Gd_3Al_2 which having a low saturation magnetization.[20] As for the x = 90 sample, magnetization increases to 90% of that X = 73.5. The reason is ascribed to the precipitated nano-sized Gd-rich crystalline having a high saturation magnetization.

Figure 3(a) displays the isothermal magnetization curves measured in a temperature range of 42-277 K under a magnetic field up to 5 T for $Gd_x(Fe_{0.566}Al_{0.434})_{100-x}$(x = 70) glassy ribbons as an example. In the vicinity of T_c, from 162 to 197 K, the temperature step is 5 K and in faraway regions of 42-162 K and 197-277 K, the temperature step is 20 K. The sweeping rate of the field was slow enough to ensure that the magnetization curves are obtained in an isothermal process. To further understand the magnetic transitions, the Arrot plots (M^2 versus H/M curves) were also analyzed. According to Banerjee criterion, a magnetic transition is considered as first-order when the slope of Arrott plot is negative; otherwise, it is expected to be second-order when the slope is positive.[21] The inflection or negative slope as an indication of metamagnetic transition above T_c is not observed in Figure 3(b), which indicates that the magnetic transition at T_c for the $Gd_x(Fe_{0.566}Al_{0.434})_{100-x}$(x = 70) alloy is a second order magnetic transition. Similarly, other $Gd_x(Fe_{0.566}Al_{0.434})_{100-x}$(x = 65-90) ternary alloys also have a nature of the second-order phase magnetic transition (not shown here).

Figure 4 shows the magnetic entropy change ΔS_M of $Gd_x(Fe_{0.566}Al_{0.434})_{100-x}$(x = 65-90) ribbons as a function of temperature under a field change of 5 T. ΔS_M for $Gd_x(Fe_{0.566}Al_{0.434})_{100-x}$(x = 65-90) ribbons was calculated in a magnetic field change of 0-5 T according to isothermal magnetization curves shown in Fig. 3 around T_c by using Maxwell relationships. The curie temperature (T_c), maximum magnetic entropy change (ΔS_M), the full width at half maximum of ΔS_M (δT_{FWHM}) and refrigeration capacity (RC) for $Gd_x(Fe_{0.566}Al_{0.434})_{100-x}$(x = 65-90) ribbons are summarized in Table I. The maximum value of ΔS_M ranges from 5.0 to 7.2 J kg^{-1} K^{-1} under a field change of 5 T for $Gd_x(Fe_{0.566}Al_{0.434})_{100-x}$(x = 65-90). These values are comparable to those of many previously published results for Gd-based crystalline and metallic glass with a second-order phase transition. For example, it has been reported that ΔS_M is ~3.7 J kg^{-1} K^{-1} (5T) for GdFeAl, ΔS_M

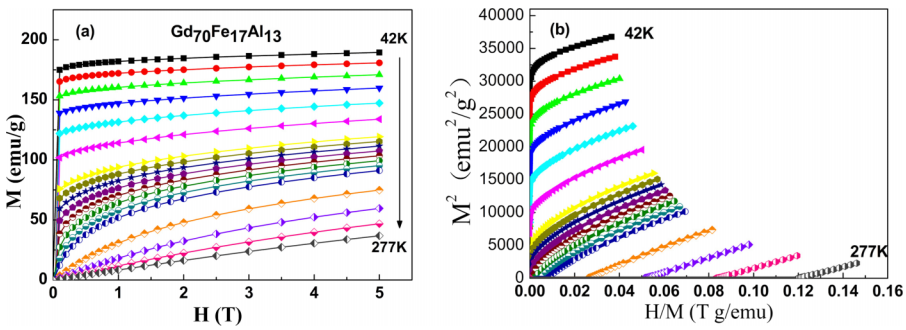

FIG. 3. Isothermal magnetization curves (a) and the Arrott plots for as-quenched $Gd_x(Fe_{0.566}Al_{0.434})_{100-x}$ (x=70) glassy ribbons as an example (b).

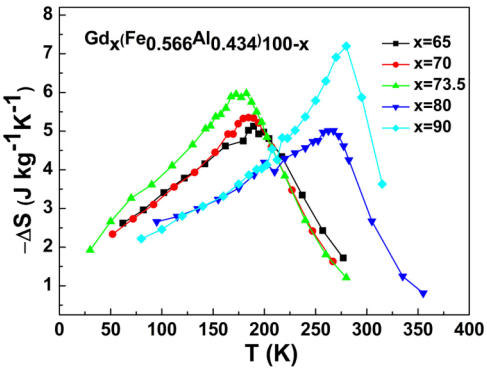

FIG. 4. Magnetic entropy changes of the $Gd_x(Fe_{0.566}Al_{0.434})_{100-x}$(x = 65-90) ribbons under a magnetic field change of 50 kOe.

is ~4.4 J kg^{-1} K^{-1} (5T) for $Gd_{60}Fe_{20}Co_{10}Al_{10}$, ΔS_M is ~10.1 J kg^{-1} K^{-1} (5T) for GdCuAl, ΔS_M is ~9.8 J kg^{-1} K^{-1} (5T) for GdCoAl.[13,22,23] All $Gd_x(Fe_{0.566}Al_{0.434})_{100-x}$(x = 65-90) alloys exhibit very high δT_{FWHM} values. The value of ΔS_M of the amorphous/nanocrystalline composite specimen with x = 80 is smaller than those of the amorphous specimens with x = 65-73.5 and Am./NC with x = 90. For higher Gd content specimens, such as Am./NC x = 90, the reason can be ascribed to the different weight percent of amorphous and nanocrystlline parts. Different weight percent of amorphous can be seen from the XRD peaks and exothermic peaks in Fig. 1(a) and 1(b). The specimen x = 90 has a higher Gd concentration and a lower content of amorphous part, thus a higher ΔS_M was obtained compared to that of x = 80. Compared with the lower Gd-containing ribbons, for example, glassy specimens, specimen x = 80 has a slightly lowered ΔS_M. The main reason is the nanocrystalline of Gd and Gd-riched compound. It was reported that with the decrease of Gd grains from micrometer to nanometer range, magnetic entropy change drops surprising from 10.07 to 4.47 J kg^{-1} K^{-1}.[24] Here, the average size of Gd_3Al_2 and Gd in x = 80 is about 20 nm, and the size of Gd in x = 90 is about 28 nm. Therefore, the nano-sized Gd has a smaller ΔS_M compared to that of bulk Gd.

It has been reported that comparing with crystalline magnetic refrigeration materials, amorphous magnetocaloric materials will exhibit higher δT_{FWHM} values due to the disordered structure resulting from their amorphous nature.[23,25] Fu *et al.*[26] have investigated the magnetic properties and ΔS_M of Gd-Co-Al glassy/compound composites and found the table-like magnetocaloric effect (MCE) by suck-casting $Gd_{52.5}Co_{16}Al_{31}$ which has a glassy structure and crystalline phases of Gd_2Al and Gd_2Co_2Al. However, Ref. 26, the table-like MCE (ΔS_M ~ 7 J kg^{-1} K^{-1}) was located between

TABLE I. Curie temperatures (T_c), the maximum magnetic entropy changes (ΔS_M), full width at half maximum of the ΔS_M (δT_{FWHM}), and refrigeration capacity (RC) of $Gd_x(Fe_{0.566}Al_{0.434})_{100-x}$(x = 65-90) ribbons at the magnetic field changes of 50 kOe and 20 kOe.

Alloy	Structure	T_c (K)	δT_{FWHM} (K)	ΔS_M (J kg^{-1} K^{-1})	RC (J kg^{-1})	Magnetic Field (kOe)
$Gd_{65}Fe_{19.8}Al_{15.2}$	Am.	192	198	5.1	761	50
	Am.	192	162	2.43	295	20
$Gd_{70}Fe_{17}Al_{13}$	Am.	182	172	5.4	690	50
	Am.	182	134	2.65	260	20
$Gd_{73.5}Fe_{15}Al_{11.5}$	Am.	172	176	5.9	789	50
	Am.	172	136	2.93	294	20
$Gd_{80}Fe_{11.3}Al_{8.7}$	Am.+NC	206/269	240	5.0	867	50
	Am.+NC	206/269	186	2.31	314	20
$Gd_{90}Fe_{5.7}Al_{4.3}$	Am.+NC	212/280	143	7.2	744	50
	Am.+NC	212/280	112	3.48	279	20

*Am. and NC stand for the amorphous and crystalline states, respectively.

47.5 K and 77.5 K. In this paper, the obtained T_c is 280 K, ΔS_M is ~7.2 J kg^{-1} K^{-1}) and δT_{FWHM} is up to 240 K, therefore, a large RC is obtained (table I).

Refrigeration capacity (RC) is another important parameter characterizing the magnetocaloric effect. The RC values can be used to calculate by a variety of methods.[23,25,27] In the present work the RC values are determined by numerically integrating the area under the ΔS_M-T curve with a full width at half maximum of the peak as the integrating limits.[28] In this work, the maximum RC value under a field change of 0-5 T reaches 867 J kg^{-1} for $Gd_{80}Fe_{11.3}Al_{8.7}$ amorphous/nanocrystalline alloy, while the minimum value is 690 J kg^{-1} for $Gd_{70}Fe_{17}Al_{13}$ alloy, which is higher than that of most classical crystalline magnetic refrigeration materials, such as Gd (556 J kg^{-1})[15] and $LaFe_{11.4}Si_{1.6}$ (439 J kg^{-1}).[28]

What is the deep reason of the Gd-based Am./NC having large magnetic entropy change than that of monolithic Gd-based metallic glass? One thing need to be mentioned is that in the inset of Figure 2, there are two peaks indicating two Curie temperatures for x = 80 alloy. And, the former was ascribed to the amorphous phase, and the latter was attributed to the Gd-riched phases, Gd_3Al_2 and Gd. The Curie temperature of the amorphous part changes with the compositional change because of the precipitated Gd-riched nanocrystalline phase, and the Curie temperature of bulk Gd_3Al_2 and bulk Gd is 281 K and 298 K, respectively.[20] However, apparently, there is only one ΔS_M peak in Figure 4, which gives a signal of combination effect of disordered part (amorphous material) and crystal part (nano-sized Gd-riched phase). In other words, amorphous part will contribute to the wider temperature range of full width at half maximum (δT_{FWHM}) and nanocrystalline will contribute to the high Curie temperature and higher magnetic entropy change. Therefore, the better comprehensive properties of Gd-based amorphous/nanocrystalline composites were obtained which is better than that of most classical crystalline magnetic refrigeration materials. And, also, our current research could shed a light on how to design and/or discover new refrigeration materials, for example, to make full use of the advantages of both amorphous and crystal materials.

IV. CONCLUSIONS

The $Gd_x(Fe_{0.566}Al_{0.434})_{100-x}$(x = 65-90) glassy alloys were prepared by the melt spinning technique at a wheel speed of 40 m/s. A magnetic second-order transition is justified by the Arrott plot for these alloys. The Curie temperature in $Gd_x(Fe_{0.566}Al_{0.434})_{100-x}$(x = 65-90) systems can be tuned from 172 to 280 K. The wide δT_{FWHM} as large as 240 K should be ascribed to the amorphous disordered structure. The large magnetic entropy change which can be tuned from 5.0 to 7.2 J kg^{-1} K^{-1} under 50 kOe was obtained for Gd-based Am./NC composites. The refrigeration capacity (RC) values of these alloys are located in the range of 690~867 J/kg under a magnetic field change of 0–5 T. The large ΔS_M and high T_c makes Gd-based amorphous/nanocrystalline composites attractive candidate for magnetic refrigeration materials at near room temperature.

ACKNOWLEDGMENTS

This work has been supported by the Natural Science Foundation of Zhejiang Province for Outstanding Youth (Grant No. LR12E01001), National Natural Science Foundation of China (Grant No. 51422106), the Natural Science Foundation of Ningbo City (Grant No. 2015A610004) and the start-up foundation of Ningbo University of Technology.

[1] K. A. Gschneidner, Jr., V. K. Pecharsky, and A. O. Tsokol, Rep. Prog. Phys. **68**, 1479 (2005).
[2] F. X. Hu, B. G. Shen, J. R. Sun, Z. H. Cheng, G. H. Rao, and X. X. Zhang, Appl. Phys. Lett. **78**, 3675 (2001).
[3] A. Fujita, S. Fujieda, Y. Hasegawa, and K. Fukamichi, Phys. Rev. B **67**, 104416 (2003).
[4] V. K. Pecharsky and K.A. Gschneidner, Jr., Phys. Rev. Lett. **78**, 4494 (1997).
[5] O. Tegus, E. Bruck, K.H.J. Buschow, and F. R. De Boer, Nature(London) **415**, 150 (2002).
[6] T. Krenke, E. Duman, M. Acet, E. F. Wassermann, X. Moya, L. Manosa, and A. Planes, Nat. Mater. **4**, 450 (2005).
[7] J. Du, Q. Zheng, W. J. Ren, W. J. Feng, X. G. Liu, and Z. D. Zhang, J. Phy. D: Appl. Phys. **40**, 5523 (2007).
[8] J. Liu, T. Gottschall, K. P. Skokov, J. D. Moore, and O. Gutfleisch, Nat. Mater. **11**, 620 (2012).
[9] Q. Luo, D. Q. Zhao, M. X. Pan, R. J. Wang, and W. H. Wang, Appl. Phys. Lett. **88**, 181909 (2006).
[10] J. Du, Q. Zheng, Y. B. Li, Q. Zhang, D. Li, and Z. D. Zhang, J. Appl. Phys. **103**, 023918 (2008).

[11] J. Du, Q. Zheng, Y.B. Li, E. Bruck, K.H.J. Buschow, W.B. Cui, W.J. Feng, and Z.D. Zhang, J. Magn. Magn. Mater. **321**, 413 (2009).
[12] F. Yuan, J. Du, and B. L. Shen, Appl. Phys. Lett. **101**, 032405 (2012).
[13] H. Fu, M. Zou, and N. K. Singh, Appl. Phys. Lett. **97**, 262509 (2010).
[14] Y. T. Wang, H.Y. Bai, M. X. Pan *et al.*, Sci China Phys Mech Astron **51**, 337 (2008).
[15] B. Schwarz, B. Podmilsak, N. Mattern, and J. Eckert, J. Magn. Magn. Mater. **322**, 2298 (2010).
[16] Z.G. Zheng, X.C. Zhong, K.P. Su, H.Y. Yu, Z.W. Liu, and D.C. Zeng, Sci China Phys Mech Astron **54**, 1267 (2011).
[17] F. Yuan, J. Li, and B.L. Shen, J . Appl .Phys. **111**, 07A937 (2012).
[18] H. Fu, M.S. Guo, H.J. Yu, and X.T Zu, J. Magn. Magn. Mater. **321**, 3342 (2009).
[19] D. Chen, A. takeuchi, and A. Inoue, J. Alloys Compd. **440**, 199 (2007).
[20] V. K. Pecharsky, K. A. Gschneidner, Jr., S. Yu Dan'kov, and A. M. Tishin, Cryocoolers **10**, 639 (1999).
[21] B. K. Banerjee, Phys. Lett. **12**, 16 (1964).
[22] Q.Y. Dong, B .G. Shen, J. Chen, J. Shen, H. W. Zhang, and J. R. Sun, J .Appl. Phys. **105**, 07A305 (2009).
[23] Q.Y. Dong, B.G. Shen, J. Chen, J. Shen, F. Wang, H.W. Zhang, and J.R. Sun, Solid State Commun. **149**, 417 (2009).
[24] H. Zeng, J. Zhang, C. Huang, and M. Yue, Appl. Nanosci. **1**, 51 (2011).
[25] Q.Y. Dong, B. G. Shen, J. Chen, J. Shen, F. Wang, H. W. Zhang, and J. R. Sun, J. Appl. Phys. **105**, 053908 (2009).
[26] H. Fu, Z. Ma, X. J. Zhang, D. H. Wang, B. H. Teng, and E. A. Balfore, Appl. Phys. Lett. **104**, 072411 (2014).
[27] M. E. Wood and W. H. Potter, Cryogenics **25**, 667 (1985).
[28] K.A. Gschneidner, Jr., V.K. Pecharsky, A.O. Pecharsky, and C.B. Zimm, Mater. Sci. Forum **69**, 315 (1999).